Fuzzy Approximation-Based Fractional-Order Nonsingular Terminal Sliding Mode Controller for DC–DC Buck Converters

Badreddine Babes, Saad Mekhilef, *Senior Member, IEEE*, Amar Boutaghane, and Lazhar Rahmani

***Abstract*—This article presents a simple and systematic approach to synthesize a robust adaptive fuzzy fractional-order nonsingular terminal sliding mode controller (AFFO-NTSMC) to improve the output voltage tracking control performance of the dc–dc buck converters. The hybrid control method of fractional-order (FO) calculus and NTSMC are combined to create a FO-NTSMC, in which a new FO nonsingular terminal sliding mode surface is established. The idea behind this strategy is the increased flexibility achieved by FO calculation, improving robustness to disturbances and parameters variations provided by the traditional sliding mode controllers as well as finite time convergence properties of the output voltage error to the equilibrium point during the output load changes, simultaneously. In addition, a fuzzy logic system with online adaptive learning algorithm is designed to provide smooth chattering in switching control signal. The stability of the closed-loop system is carefully demonstrated by Lyapunov's theorem. Experimental measurements from a laboratory prototype are presented to demonstrate the effectiveness of the proposed AFFO-NSTSMC algorithm.**

***Index Terms*—Adaptive fuzzy logic system, chattering reduction, dc–dc buck converter, finite time convergence, fractional-order calculus, fractional-order nonsingular terminal sliding mode control (FO-NTSMC).**

I. Introduction

FOR MANY years, serious efforts have been devoted to the control of the dc–dc buck (step-down) converter, because of its importance in various industrial applications that require high precision in output voltage measurement and good dynamic response of the output current, such as auxiliary power sources in electric vehicles [1], dc motor drives, communication equipment, computers, and automotive systems [2]–[4]. However, the dc–dc buck converter entails inherent uncertainties and nonlinearities produced by the model plant mismatches, external disturbances, electro-magnetic interference, etc., which makes the control of the dc–dc buck converter very complicated and causes a steady-state error in the output voltage response.

Early control efforts for those dc–dc converters have contributed to the linear control methods based on linearized models, which have proved their capability, but the control performances easily deteriorate under various disturbances in the dc–dc power conversion systems [5]. Therefore, to achieve better control performance for these converters, a high-performance controller for a dc–dc buck converter is required to have a satisfactory disturbance rejection capability, a small steady-state error, a fast dynamic response, and minimal overshoots in various aspects. Thus, the nonlinear control methods are considered as a natural control to satisfy the dc–dc buck converter output voltage requirements, and more appropriate when compared with the linear control methods.

Numerous advanced nonlinear control techniques have been developed, such as backstepping control [6], adaptive control [7], proximate time-optimal control [8], sliding mode control (SMC) [9], hierarchical control [10], synergetic control [11], and neural network control [12]. These nonlinear control techniques can improve the performance of dc–dc buck converter circuits in different industrial applications. Among the nonlinear control techniques, the SMC method has received a great deal of attention because of its main advantages, which are a simple structure, high robustness against a variety of parameter uncertainties, and external disturbance [13], [14]. The SMC, which was introduced for controlling variable structure systems is considered to be an effective control scheme for both linear/nonlinear systems, and certain/uncertain systems for its insensitivity to parameter uncertainties [15]. By inheriting these advantages, SMC has been developed diversely to pulsewidth-modulation (PWM) based SMC [16], [17], double-integral SMC [18], second-order SMC [19], [20], discrete SMC [21] for buck converter systems, electrical drive systems, and wind energy conversion systems. In conventional SMC, a linear sliding surface is chosen which only guarantees asymptotic stability of the system in a sliding

Manuscript received April 8, 2021; revised July 31, 2021; accepted September 5, 2021. Date of publication September 22, 2021; date of current version November 30, 2021. This work was supported in part by the High Impact Research of the Research Center in Industrial Technologies and in part by the Ministry of Higher Education, Malaysia for the financial support under the Long Term Research Grant Scheme (LRGS) under Grant LRGS/1/2019/UKM-UM/01/6/3. Recommended for publication by Associate Editor T. Suntio. *(Corresponding author: Saad Mekhilef.)*

Badreddine Babes and Amar Boutaghane are with Research Center in Industrial Technologies, Algiers 16014, Algeria (e-mail: elect_babes@yahoo.fr; aboutaghane@yahoo.fr).

Saad Mekhilef is with the Swinburne University of Technology, Hawthorn, VIC 3122, Australia, and also with Power Electronics and Renewable Energy Research Laboratory, Department of Electrical Engineering, Faculty of Engineering, University of Malaya, Kuala Lumpur 50603, Malaysia (e-mail: saad@um.edu.my).

Lazhar Rahmani is with the Department of Electrical Engineering, Faculty of Technology, University of Setif-1, Setif 390001, Algeria (e-mail: lazhar_rah@yahoo.fr).

Color versions of one or more figures in this article are available at https://doi.org/10.1109/TPEL.2021.3114277.

Digital Object Identifier 10.1109/TPEL.2021.3114277

phase. In particular, no matter how the parameters of the sliding surface are adjusted, it is impossible for the system states to reach the equilibrium point in a restricted time [22]. In addition, the uncontrollable infinite switching frequency caused by the sign function of the control law cannot be avoided [14]. To address this dilemma, the terminal SMC (TSMC) schemes with a nonlinear sliding surface have been developed in [14] and [22], which accomplishes some excellent properties, such as faster finite-time convergence, better tracking accuracy, and stronger robustness regarding uncertainties and external disturbances compared to conventional SMC [23]. For the TSMC strategy, Komurcugil *et al.* [24] indicated that an exponential factor could be introduced into the sliding surface to accomplish a dynamic adjustment for the feedback of the output voltage error. If an appropriate exponential factor is designed, it can improve the convergence time. However, there still exist defects in traditional TSMC strategy; notably the singularity problem [14], and the requirement for prior knowledge of nonlinear system dynamics [25]. As a result, the equivalent control part of the traditional TSMC strategy might be uncontrollable. Therefore, to effectively avoid the singularity problems, a nonsingular TSMC (NTSMC) has been presented in [14] and [26]. The NTSMC controller can solve the singular problem, but the upper bounds of the external disturbances and uncertainties usually must be known for calculating the switching gain [27], which might be unavailable in real time.

The adaptive concept is an effective method to deal with these unknown external disturbances and uncertainties by estimating the upper bounds of them [28]. In many past studies [29], [30], adaptive control techniques have successfully advanced in tackling control problems for uncertain nonlinear systems. To allow the controlled system to realize finite-time convergence even in the condition of unknown boundary disturbances and overcome the singular problem in designing TSMC synchronously, a kind of adaptive estimation method was incorporated into NTSMC. To reduce the chattering caused by SMC, the switching part in the controller was removed. In [30], an adaptive NTSMC algorithm has been proposed to control an autonomous underwater vehicle. In [31], a robust adaptive terminal sliding mode synchronized algorithm was introduced for a class of nonautonomous chaotic systems. In [32], an adaptive NTSMC algorithm was proposed using fuzzy wavelet networks to approximate the unknown dynamics of robots with an adaptive learning algorithm. Adaptive NTSMC controllers were introduced for the microgyroscope in [33] and [34].

A switching SMC strategy is applied not only to integer-order systems but also to fractional-order (FO) ones [35]. Fractional order calculus is an extension of integer-order differentiation and integration to FO ones, which can date back to the end of the 17th century, when Leibniz and Newton invented differential calculus [36]. Recently, more and more attention has been focused on its application in industrial control systems rather than a pure theoretical mathematical subject due to its higher control accuracy, an extra degree of freedom and powerful tools of analysis, modeling and control of natural and industrial systems in comparison with integer-order controllers. It is merit mentioning the control of a dc motor [37], control of a bioreactor [38], MPPT control of PV systems [39], control of insulin-glucose [40], and robot trajectory planning [41], as some applications of FO control.

Recently, FO calculus has been combined into SMC controller design for FO systems and their integer-order counterpart, which provides both merits simultaneously. Chen *et al.* [42] proposed an adaptive SMC for a class of FO nonlinear systems with uncertainties. Yin *et al.* [43] designed an adaptive sliding mode controller for both integer and FO chaotic systems with uncertainty and external disturbance to realize chaos control, which has shown a supplementary degree of freedom in a fractional sliding surface. Lin *et al.* [44] dealt with chaos synchronization between two different uncertain FO chaotic systems based on adaptive fuzzy sliding mode control. Nojavanzadeh and Badamchizadeh [45] proposed an adaptive FO NTSMC for robot manipulators with uncertainties solved by adaptive tuning methods, which ensured finite-time convergence and better tracking performance.

An adaptive fuzzy SMC with a fractional-order integration scheme was presented in [46] to adjust the parameter, which can show better tracking performance and a higher degree of robustness to disturbances compared to conventional integer order ones. An adaptive FO sliding controller with a neural estimator was discussed in [47]. However, there are few previous works considering the application of FO-NTSMC for an integer-order system with uncertainties. The combination of NTSMC controller with FOs calculus for the dc–dc buck converter can improve the tracking performance and stabilize the output voltage in a short period of time. It is a very interesting work to combine adaptive fuzzy NTSMC controller with FO calculus for dc–dc buck converter systems together, which has not been studied so far in the literature. Motivated by the abovementioned advantages, an adaptive fuzzy fractional-order nonsingular terminal sliding mode control (AFFO-NTSMC) algorithm is proposed for a dc–dc buck converter in this paper. The sliding surface is a FO nonsingular terminal sliding surface, and the dynamics of the dc–dc buck converter is described by integer-order not fractional-order.

The FO-NTSMC algorithm is used to make the dc–dc buck converter reach steady-state within a limited time, and a fuzzy adaptive law is integrated with the FO-NTSMC control scheme to make the proposed control scheme have adaptive ability to disturbances, and overcome the limitation on FO-NTSMC control method caused by disturbance boundary value. Based on the above-mentioned consideration and analysis, the main contributions of this article can be highlighted in four aspects as follows. First, the superior characteristic of the proposed control method is that a FO derivative term is adopted in the sliding manifold, which generates an additional degree of freedom on the NTSM surface, so that the performance of the proposed controller can be significantly improved. Second, the NTSM surface chosen in the proposed controller design provides the finite-time convergence without singularity. Third, a dynamic adaptive fuzzy term is introduced in the designing of FO-NTSMC control law to estimate the upper bound of the lumped uncertainties of the system. This scheme can bring the dc–dc buck converter to achieve steady-state quickly without chattering, and have good robustness to external disturbances and internal parameter variations. Fourth, the entire adaptive

fuzzy NTSMC control strategy with FOs (AFFO-NTSMC) is also derived in the sense of Lyapunov stability theory to ensure the stability of the dc–dc buck converter system, while improving the output voltage regulation performance and stabling it in a short time.

The rest of this article is organized as follows. Section II introduces some necessary preliminary definitions and basic concepts related to fractional-order calculus and fuzzy logic systems. Section III presents the fundamental problem regarding dc–dc buck converter system and its simplified model. Section IV describes the explicit control law construction procedure of the FO-NTSMC algorithm and the AFFO-NTSMC algorithm. In Section V, the performance of the proposed AFFO-NTSMC algorithm is verified by running experiments on the dc–dc buck converter. Finally, Section VI concludes this article.

II. Preliminaries of Fractional Calculus and Fuzzy Logic

A. Concepts of Fractional Calculus

Fractional calculus is a generalization of conventional integral calculus. Compared with IO calculus, FO calculus has more universal significance.

There are three common definitions of FO calculus [48]–[50]; Riemann–Liouville (RL), Grunwald–letnikov (GL), and Caputo, which are expressed as follows.

1) RL Definition

$$ {}_bD_t^{\alpha} f(t) = \frac{d^{\alpha} f(t)}{dt^{\alpha}} = \frac{1}{\Gamma(n-\alpha)} \frac{d^n}{dt^n} \int_b^t \frac{f(\tau)}{(t-\tau)^{\alpha-n+1}} d\tau. \tag{1} $$

2) GL Definition

$$ {}_bD_t^{\alpha} f(t) = \lim_{k \to 0} h^{-\alpha} \sum_{j=0}^{\infty} (-1)^j \binom{\alpha}{j} (t - jh). \tag{2} $$

In (1) and (2), *n-1*$<\alpha \leq n$. ${}_{t_0}D_t^{\alpha} f(t)$is the a -order differential of $f(t), t_0$ and t are the bounds of the operator ${}_{t_0}D_t^{\alpha}$, and $\Gamma(.)$ is the popular Gamma function which is defined as: $\Gamma(\alpha) = \int_0^{\infty} \exp(-t) t^{\alpha-1} dt$, h is the calculation step size.

3) Caputo Definition

$$ {}_bD_t^{\alpha} f(t) = \frac{1}{\Gamma(n-\alpha)} \int_{t_0}^t \frac{f^{(n)}(\tau)}{(t-\tau)^{\alpha-n+1}} d\tau. \tag{3} $$

B. Concepts of Fuzzy Logic

Fuzzy logic system (FLS) has the universal approximation property that states that any sufficiently smooth function can be approximated by a suitable MIMO-FLS for all inputs in a compact set and the resulting function reconstruction error is bounded. A MIMO-FLS system with center-average defuzzifier, product inference, and singleton fuzzifier is given by following relation [51]:

$$ y_j = \frac{\sum_{l=1}^{M} \mu_{A_i^l}(x_i) \overline{y}_j^l}{\sum_{l=1}^{M} \mu_{A_i^l}(x_i)}, \quad j = 1, 2, \ldots, m. \tag{4} $$

Here, x_i is the input parameter vector, y_j is the output parameter vector, M represents the total number of rules, and $\mu_{A_i^l}(x_i)$ is the membership function vector. Equation (4) can be rewritten as

$$ y_j = \theta_j \, \zeta(x), \quad j = 1, 2, \ldots, m. \tag{5} $$

Here, θ_j is the parameter vector which is adaptive term, $\zeta(x)$ is fuzzy basis function vector, and $\overline{y}_j^l$is a free parameter.

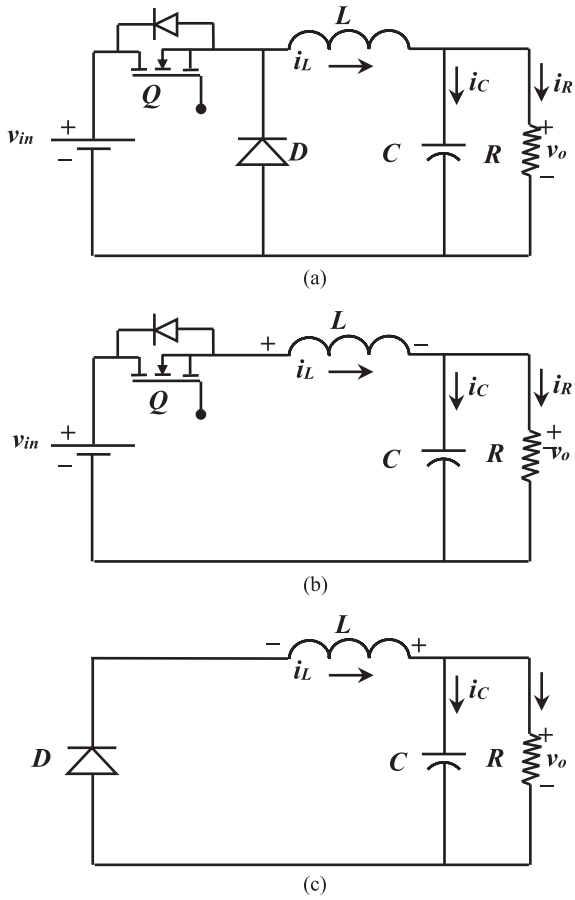

Fig. 1. Diagram of the dc–dc buck converter circuit. (a) Case of the average mode, (b) case when the switch (Q) is ON, and (c) case when the switch (Q) is OFF.

III. Problem Description

The dc–dc buck converter circuit usually comprises of a dc voltage source (v_{in}), a controllable switch (Q), a diode (D), an inductor (L), a capacitor (C) and a load resistor (R), properly connected, as in Fig. 1. The switch ON/OFF (activation/deactivation)

conditions of the dc–dc buck converter circuit is illustrated by Fig. 1(b) and (c), respectively.

When the switch Q is turned ON, the operation of the dc–dc buck converter can be described as

$$\frac{di_L}{dt} = \frac{1}{L}\left(v_{in} - v_0\right), \qquad \frac{dv_0}{dt} = \frac{1}{C}\left(i_L - \frac{v_0}{R}\right). \quad (6)$$

When the switch Q is turned OFF, the operation of the dc–dc buck converter can be described as

$$\frac{di_L}{dt} = -\frac{v_0}{L}, \qquad \frac{dv_0}{dt} = \frac{1}{C}\left(i_L - \frac{v_0}{R}\right). \quad (7)$$

Combining (6) and (7), we obtain the averaged model as follows:

$$\frac{di_L}{dt} = \frac{1}{L}\left(u\, v_{in} - v_0\right), \qquad \frac{dv_0}{dt} = \frac{1}{C}\left(i_L - \frac{v_0}{R}\right) \quad (8)$$

where u is the control input, called duty ratio

Consider that the effect of disturbances caused by parametric uncertainties and external disturbances may occur in running processes, the dynamic system in (8) can be amended as follows:

$$\begin{aligned}\frac{di_L}{dt} &= \frac{u(t)(v_{in} + \Delta v_{in}) - v_0}{L + \Delta L} + d(t),\\ \frac{dv_0}{dt} &= \frac{i_L - (v_0/(R + \Delta R))}{C + \Delta C}\end{aligned} \quad (9)$$

where the parameters $\Delta v_{in},\ \Delta L,\ \Delta R$, and $d(t)$ are parameter perturbations, while $d(t)$ represents the corresponding system uncertainty and external disturbance. It is assumed that $d(t)$ and $\dot{d}(t)$ are both bounded, and the system (9) can be transformed to the following form:

$$\begin{aligned}\frac{di_L}{dt} &= \frac{u(t)\, v_{in} - v_0}{L} + L_1(e,t)\\ \frac{dv_0}{dt} &= \frac{i_L - (v_0/R)}{C} + L_2(e,t)\end{aligned} \quad (10)$$

where $L_1(e,t)$ and $L_2(e,t)$ are expressed as

$$\begin{aligned}L_1(e,t) &= \tfrac{u(t)\,\Delta v_{in} L - u(t)\,\Delta L v_{in} + \Delta L v_0}{(L+\Delta L)L} + d(t)\\ L_2(e,t) &= \tfrac{v_0 \Delta R}{R(R+\Delta R)(C+\Delta C)} + \tfrac{v_0 \Delta C - i_L \Delta C R}{CR(C+\Delta C)}.\end{aligned} \quad (11)$$

Since $d(t),\ \Delta v_{in},\ \Delta R,\ \Delta L$, and ΔC are all bounded, this implies that $L_1(e,t)$ and $L_2(e,t)$ are also bounded.

Define the output voltage error e_1 as follows:

$$e_1 = v_0 - v_{ref} \quad (12)$$

where v_{ref} denotes the reference value of the dc output voltage. By taking the time derivative of (12), e_2 which is the rate of change of voltage error can be expressed as

$$\dot{e}_1 = e_2 = \dot{v}_0. \quad (13)$$

Then, the dynamics of e_2 can be given as

$$\dot{e}_2 = \frac{1}{LC}\left(u(t)\, v_{in} - v_{ref} - e_1\right) - \frac{e_2}{RC} + L(e,t). \quad (14)$$

So, the controlled state variables of dc–dc buck converter are selected as follows:

$$\begin{cases}\dot{e}_1 = e_2\\ \dot{e}_2 = u(t)\frac{v_{in}}{LC} - \frac{v_{ref}}{LC} - \frac{e_1}{LC} - \frac{e_2}{RC} + L(e,t)\end{cases} \quad (15)$$

where the system disturbance $L(e,t)$, which the dc–dc buck converter can endure includes both $L_1(e,t)$ and $L_2(e,t)$ and can be expressed as

$$L(e,t) = \frac{L_1(e,t)}{C} - \frac{L_2(e,t)}{RC} + \dot{L}_2(e,t). \quad (16)$$

For the controller design, we set the following simplification:

$$b_n(e,t) = \frac{v_{in}}{LC}, \text{ and} f_n(e,t) = \frac{v_{ref}}{LC} + \frac{e_1}{LC} + \frac{e_2}{RC}$$

Then, the dynamical model (16) of dc–dc buck converter can be described as

$$\begin{cases}\dot{e}_1 = e_2\\ \dot{e}_2 = u(t)\, b_n(e,t) - f_n(e,t) + L(e,t).\end{cases} \quad (17)$$

The objective of this article is to design a control law limited between 0 and 1, representing the duty ratio, allowing the dc–dc buck converter to switch between two topologies in the continuous conduction mode (CCM) by achieving a tracking reference voltage (v_{ref}). Furthermore, since the dc–dc buck converter is nonlinear, the followed approach thereafter is the so-called AFFO-NTSMC.

IV. Control Design

A. Design of FO-NTSMC Controller

FO-NTSMC introduces the fractional calculus term into traditional SMC, and its design is similar to that of traditional SMC. To design a FO-NTSMC for dc–dc buck converter system (17), first, we propose the following FO nonsingular sliding mode surface function using Reimann–Liouville's definition as follows:

$$s = {}_{t_0}D_t^{\alpha} e_1 + \frac{1}{\rho} sgn(e_2)^{\lambda} \quad (18)$$

where ${}_{t_0}D_t^{\alpha}$ is the fractional derivative of order α that satisfies $0 < \alpha < 1$, and ρ is a designed positive constant, p and q are positive odd numbers that satisfies $1 < \lambda = (p/q) < 2$, and $sgn(.)^{\lambda} = |.|^{\lambda} sgn(.)$.

By (17) and (18), the dynamics of the sliding variable s can be written as

$$\begin{aligned}\dot{s} = {}_{t_0}D_t^{\alpha+1} e_1 + \frac{\lambda}{\rho}\dot{e}_2 |e_2|^{\lambda} = {}_{t_0}D_t^{\alpha+1} e_1 + \frac{\lambda}{\rho}|e_2|^{\lambda-1}\\ \times \left[\frac{1}{LC}\left(u(t)\, v_{in} - v_{ref} - e_1\right) - \frac{e_2}{RC} + L(e,t)\right].\end{aligned} \quad (19)$$

After establishing the derivative of the manifold, the next step is to design the equivalent control law for dc–dc buck converter. By setting $\dot{s} = 0$, the equivalent control law can be obtained as

$$u_{eq}(t) = \frac{LC}{v_{in}}\left[\frac{v_{ref}}{LC} + \frac{e_1}{LC} + \frac{e_2}{RC} - \frac{\rho}{\lambda}{}_{t_0}D_t^{\alpha+1} e_1 |e_2|^{1-\lambda}\right]. \quad (20)$$

The switching control law for dc–dc buck converter can be obtained as

$$u_{sw}(t) = -\frac{LC}{v_{in}}\left[K_1 s + K_2\, sgn(s) + \delta\right],\ K_1 > 0,\ K_2 > 0 \quad (21)$$

where $u_{sw}(t)$ is the robust switching control element to handle the lumped uncertainty $L(e,t)$. In (21), to reach and maintain the sliding surface in finite time at any initial state, K_1 and K_2 were greater than 0. The global control law can be obtained by combining (20) with (21) as follows:

$$\begin{aligned} u(t) &= u_{eq}(t) + u_{sw}(t) \\ &= \frac{LC}{v_{in}}\left[\frac{v_{ref}}{LC} + \frac{e_1}{LC} + \frac{e_2}{RC} - \frac{\rho}{\lambda} t_0 D_t^{\alpha+1} e_1 |e_2|^{1-\lambda}\right. \\ &\quad \left. - (K_1 s + K_2\, sgn(s) + \delta)\right]. \end{aligned} \tag{22}$$

B. Design of AFFO-NTSMC Controller

For FO-NTSMC controller, the chattering suppression effect is limited if its switching control law is attenuated because the output voltage fluctuations of the dc–dc buck converter are large when the input voltage or load resistor was abrupt. Therefore, an AFFO-NTSMC controller is used to reduce the impact of chattering and convergence time. Simultaneously, it is difficult to establish a precise model to approximate $K_2\, sgn(s)$value because the dc–dc buck model parameter mismatches and dc source voltage variations cannot be determined. Fuzzy system does not require complex mathematical models, and the relevant control behavior laws can be solidified into fuzzy control rules. Therefore, in this article, we use an adaptive fuzzy control system $\hat{h}(s|\theta)$ to approximate the $K_2\, sgn\,(s)$ value online.

Ideal output of the fuzzy system is as follows:

$$\hat{h}\,(s|\,\theta) = \theta^T \zeta(s) \tag{23}$$

where $\hat{h}(s|\theta)$ is the estimated value of $K_2\, sgn\,(s)$, $\theta = [\theta_1, \theta_2, \ldots, \theta_m]^{\mathrm{T}}$ is the actual adjustable parameters which is updated online all the time, $\zeta(s) = [\zeta_1, \zeta_2, \ldots, \zeta_{\mathrm{m}}]^{\mathrm{T}}$ is fuzzy basis function is given by $\zeta(s) = \frac{(\prod_{i=1}^{n} \mu_j(s_i))}{\sum_{j=1}^{m}(\prod_{i=1}^{n} \mu_j(s_i))}$, and m refers to the number of membership functions, μ_j are the membership functions.

Assuming that the fuzzy vector of the optimal approximation parameter θ^* defined as

$$\theta^* = \arg\min_{\theta \in \Omega_0}\left(Sup_{s \in \Omega_1}\left|\hat{h}\,(s|\,\theta) - K_2\, sgn(s)\right|\right) \tag{24}$$

where Ω_0 and Ω_1 are the bounded set of θ and s, respectively. Sup (.) represents the minimum upper bound of $\hat{h}(s|\theta)$ and arg min (.) is the set of value of s for which $\hat{h}(s|\theta)$ has the largest value. When θ gets the optimal constant θ^*, $\hat{h}(s|\theta)$ turns into

$$\hat{h}\,(s|\,\theta) = \theta^{*T} \zeta(s). \tag{25}$$

Such that the approximation of $K_2\, sgn(s)$ is most accurate. This yields the minimum approximation error for the fuzzy system as

$$\omega(s) = \hat{h}\,(s|\,\theta) - \theta^{*T} \zeta(s) \tag{26}$$

when θ gets the optimal parameter $\theta*$, $\hat{h}(s|\theta)$turns into

$$\hat{h}\,(s|\,\theta^*) = K_2\, sgn(s). \tag{27}$$

Based on the universal approximation theorem [52], for a positive unknown constant there exists

$$\left|K_2\, sgn(s) - \theta^{*T} \zeta(s)\right| = |\omega(s)| \le \omega_{\max}(s). \tag{28}$$

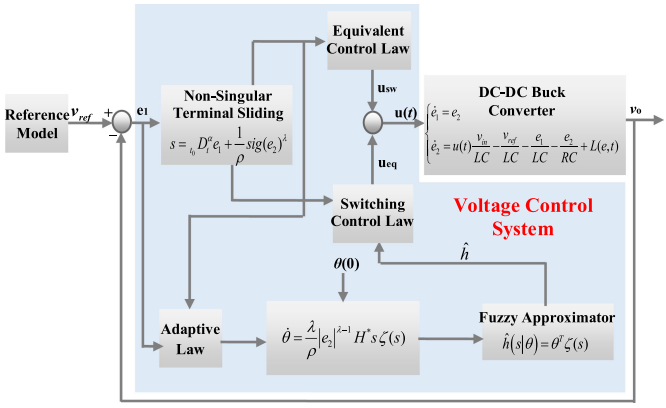

Fig. 2. Schematic diagram of AFFO-NSTSMC controlled system.

Therefore, to stabilize the uncertain nonlinear system (17) in the presence of external disturbances and uncertainties, an AFFO-NTSMC control law can be designed as follows:

$$\begin{aligned} u(t) = \frac{LC}{v_{in}}\left[\frac{v_{ref}}{LC} + \frac{e_1}{LC} + \frac{e_2}{RC} - \frac{\rho}{\lambda} t_0 D_t^{\alpha+1} e_1 |e_2|^{1-\lambda}\right. \\ \left. - \left(K_1 s + \hat{h}\,(s\,|\theta^*) + \delta\right)\right]. \end{aligned} \tag{29}$$

The schematic diagram of AFFO-NTSMC for a dc–dc buck converter is designed in Fig. 2, and the tracking error comes to the proposed controller. The designed controller has three parts, 1) adaptive system is used to learn the unknown dynamics, 2) fuzzy approximator is developed to attenuate the effect of uncertainties and disturbance, and 3) robust FO-NSTSM control is utilized to improve the tracking performance. First, $s\,\dot{s}$is designed as the input variable of fuzzy rules. Then, the adaptive law can be applied, and the output of adaptive fuzzy logic system $\hat{h}$ is obtained through (25). Finally, the AFFO-NSTSM controller is determined from (29).

C. Design of Fuzzy Approximator

In this section, the design steps of the fuzzy approximator will be explained in detail. The block diagram of the proposed method composed of the AF-FONTSMC controller and fuzzy approximator is given in Fig. 3.

In the AFFO-NSTSMC, the input and output vectors of fuzzy logic approximator have the same type of member functions that are all Gaussian membership functions formulated as $\mu_h = \exp\left[-(x + 4 - 1.6(i-1))^2\right]$, $i = 1, \ldots, 7$, which is shown in Fig. 4. The adaptive fuzzy parameters are selected as follows:$\theta = [\theta_1\ \theta_2\ \theta_3\ \theta_4\ \theta_5\ \theta_6\ \theta_7]$.

The first step is to design the fuzzy rules

IF $s\,\dot{s} < 0$, THEN $K_2\, sgn(s)$should be reduced.

Fuzzy system of $s\,\dot{s}$ and $K_2\, sgn(s)$can be designed according to formula (27). We stipulate $s\,\dot{s}$ is Input and $\hat{h}$is Output. Using seven-level fuzzy sets, their definitions are as follows:

$$s\,\dot{s} = \{NBNMNSZEPSPMPB\}$$

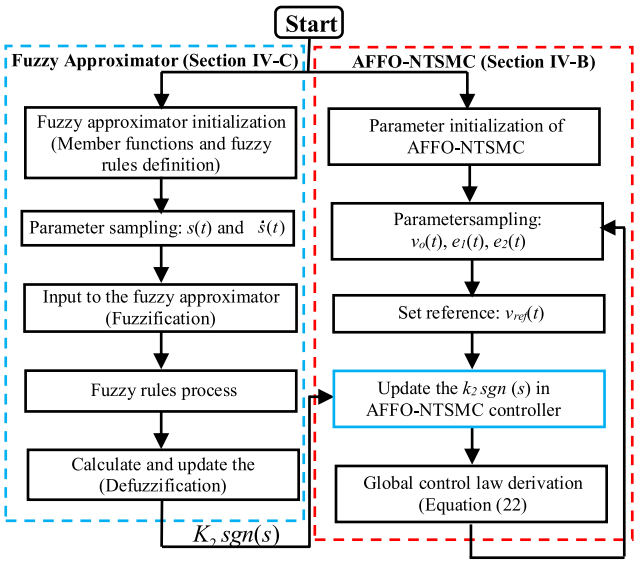

Fig. 3. Implementation of the AF-FONTSMC controller.

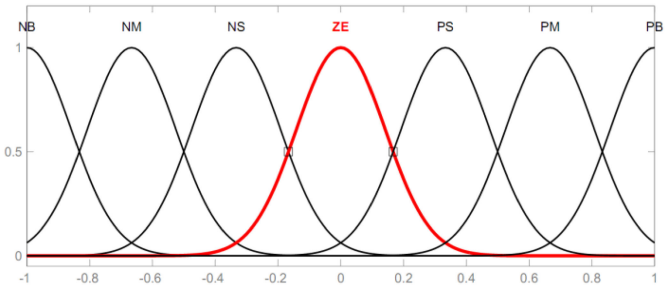

Fig. 4. Membership functions of x.

$$\hat{h} = \{NBNMNSZEPSPMPB\}.$$

The Mamdani-type fuzzy inference can easily design the $K_2\, sgn(s)$as a controller because its rule is more in line with language expression. Here, a fuzzy approximator was designed using the Mamdani fuzzy system. In the fuzzy approximator, we can define a set of seven membership functions uniformly distributed on a universe of discourse [–1, 1]. The fuzzy set [Negative Big (NB), Negative-Medium (NM), Negative Small (NS), Zero (ZE), Positive Small (PS), Positive-Medium (PM), and Positive Big (PB)] is the input and output of the fuzzy approximator. The fuzzy rules for $\hat{h}$ can be summarized as follows:

R1: IF $s\,\dot{s}$is PB, THEN $\hat{h}$ is PB
R2: IF $s\,\dot{s}$ is PM, THEN $\hat{h}$ is PM
R3: IF $s\,\dot{s}$ is PS, THEN $\hat{h}$ is PS
R4: IF $s\,\dot{s}$ is ZE, THEN $\hat{h}$ is ZE
R5: IF $s\,\dot{s}$ is NS, THEN $\hat{h}$ is NS
R6: IF $s\,\dot{s}$ is NM, THEN $\hat{h}$ is NM
R7: IF $s\,\dot{s}$ is NB, THEN $\hat{h}$ is NB.

The fuzzy outputs cannot directly affect the system, and they must be defuzzified. Compared with other defuzzification methods, the centroid method has a smoother output inference control effect, and the outputs change, even if it corresponds to a small change in input. Therefore, in this article, the centroid defuzzification method was adopted. Using this method, the corresponding change$\Delta\hat{h}$ for the $K_2\, sgn(s)$ can be calculated using

$$\Delta\hat{h} = \frac{\sum_{i=1}^{7}\theta_i\mu_i(s\dot{s})\mu_i(s\dot{s})}{\sum_{i=1}^{7}\mu_i(s\dot{s})\mu_i(s\dot{s})} = \frac{\sum_{i=1}^{7}\theta_i\zeta_i}{\sum_{i=1}^{7}\zeta_i}$$
$$= [\theta_1 \ldots \theta_7]\begin{bmatrix}\zeta_1\\ \vdots\\ \zeta_7\end{bmatrix} / \sum_{i=1}^{7}\zeta_i = \theta^T\zeta(s\dot{s}) \tag{30}$$

where μ_i represents the weight of the ith rule. The modified $\hat{h}$ can be used to update the AFFO-NTSMC controller to suppress the output voltage oscillations in the dc–dc buck converter.

D. Stability Analysis

To analyze the system stability, the Lyapunov candidate function was applied. The sliding surface (s) is a function of the system state for dc–dc buck converter, and thus, the system stability can be judged by the Lyapunov function composed of sliding surface (s). We take the positive definite scalar function (V) as the Lyapunov function

$$V = \frac{1}{2}\left(s^2 + H^{*-1}\tilde{\theta}^T\tilde{\theta}\right) \tag{31}$$

where $H^* > 0$ is an update gain. Let $\tilde{\theta} = \theta^* - \hat{\theta}$ be the approximation error where $\hat{\theta}$ the estimated value of θ^*

$$\dot{\tilde{\theta}} = \dot{\theta}^* - \dot{\hat{\theta}} = -\dot{\hat{\theta}}. \tag{32}$$

The adaptive update law of the fuzzy logic system is set as

$$\dot{\theta} = \frac{\lambda}{\rho}|e_2|^{\lambda-1}H^* s\,\zeta(s). \tag{33}$$

Making the time derivative of V obtains

$$\dot{V} = s\,\dot{s} + H^{*-1}\,\tilde{\theta}^T\,\dot{\tilde{\theta}}$$
$$= s\left[{}_{t_0}D_t^{\alpha+1}e_1 + \frac{\lambda}{\rho}|e_2|^{\lambda-1}\left[\frac{1}{LC}\left(u(t)\,v_{in} - v_{ref} - e_1\right)\right.\right.$$
$$\left.\left. - \frac{e_2}{RC} + L(e,t)\right]\right] + H^{*-1}\tilde{\theta}^T\dot{\tilde{\theta}}. \tag{34}$$

Inserting (23) and (31) into (34) results in

$$l\dot{V} = s\frac{\lambda}{\rho}|e_2|^{\lambda-1}\left(L(e,t) - \left(K_1 s + \theta^T\zeta(s) + \delta\right)\right)$$
$$+ s\frac{\lambda}{\rho}|e_2|^{\lambda-1}\tilde{\theta}^T\zeta(s) \le \sigma\frac{\lambda}{\rho}|e_2|^{\lambda-1}$$
$$\left(-K_1\sigma - \theta^{*T}\zeta(\sigma) - \theta^T\zeta(\sigma) - \theta^{*T}\zeta(\sigma)\right) + \sigma\frac{\lambda}{\rho}|e_2|^{\lambda-1}\tilde{\theta}^T\zeta(\sigma)$$
$$\le s\frac{\lambda}{\rho}|e_2|^{\lambda-1}\left(-K_1 s - \tilde{\theta}^T\zeta(s) - \theta^{*T}\zeta(s)\right) + s\frac{\lambda}{\rho}|e_2|^{\lambda-1}\tilde{\theta}^T\zeta(s)$$
$$\le s\frac{\lambda}{\rho}|e_2|^{\lambda-1}\left(-K_1 s - \theta^{*T}\zeta(s)\right). \tag{35}$$

Because $\theta^{*T}\zeta(s) = K_2\, sign(s)$, we can get

$$\dot{V} \leq s\frac{\lambda}{\rho}|e_2|^{\lambda-1}\left(-K_1 s - K_2\, sgn(s)\right). \tag{36}$$

Therefore,

$$\dot{V} \leq \frac{\lambda}{\rho}|e_2|^{\lambda-1}\left(-sK_1 s - K_2\ |s|\right) < 0\ . \tag{37}$$

From (67) and according to Lyapunov stability theorem, the dc–dc buck converter with the AFFO-NTSMC is stable.

E. Arrival Time Analysis

In Section IV-D, it is found that the dc–dc buck converter is stable under the reaching law (29), and to derive the arrival time to the sliding surface, fractional-integral of both sides of (18) is applied from t_r to t

$$\begin{aligned} {}_{t_r}D_t^{-\alpha}({}_{t_r}D_t^{\alpha}e_1) &= e_1 - \left({}_{t_r}D_t^{\alpha-1}e_1\big|_{t=t_r}\frac{(t-t_r)^{\alpha-1}}{\Gamma(\alpha)}\right) \\ &= -\frac{1}{\rho}{}_{t_r}D_t^{-\alpha}|e_2|^{\lambda} \end{aligned} \tag{38}$$

where ${}_{t_r}D_t^{\alpha-1}e_1|_{t=t_r}(\frac{(t-t_r)^{\alpha-1}}{\Gamma(\alpha)}) = 0$.

Using the property of norm, i.e., $\|\phi.\vartheta\| = \|\phi\|\|\vartheta\|$, for $\phi \in R$, and the result of Property, i.e., $\|{}_{t_r}D_t^{-\alpha}|e_2|^{\lambda}\| \leq \psi\||e_2|^{\lambda}\|$.

We obtain

$$\|e_1\| \leq \frac{\psi}{\beta}\left\||e_2|^{\lambda}\right\| \leq \frac{\psi}{\beta}\|e_2\|^{\lambda} \tag{39}$$

where ψ and β are the positive constants. Taking the integer order integral of both sides of (38) from the reaching time $t_r$to $t_s \in [t_r, +\infty[$, one obtains

$$\begin{aligned} \left|\int_{t_r}^{t_s}\left(\frac{\beta}{\psi}\right)^{\frac{1}{\lambda}}d\sigma\right| &\leq \left|\int_{t_r}^{t_s}\frac{d(\|e_1(\sigma)\|)}{\|e_1(\sigma)\|^{\frac{1}{\lambda}}}\right| \Rightarrow t_s - t_r \\ &\leq \left(\frac{\psi}{\beta}\right)^{\frac{1}{\lambda}}\left[\frac{\lambda}{\lambda-1}\right]\left|\|e_1(t_s)\|^{\left(1-\frac{1}{\lambda}\right)} - \|e_1(t_r)\|^{\left(1-\frac{1}{\lambda}\right)}\right|. \end{aligned} \tag{40}$$

Noting that $e_1 = 0$ at $t = t_s$. Therefore, the arrival time $t_s$can be obtained as

$$t_s \leq \left(\frac{\psi}{\beta}\right)^{\frac{1}{\lambda}}\left[\frac{\lambda}{\lambda-1}\right]\left[\|e_1(t_r)\|^{\left(1-\frac{1}{\lambda}\right)}\right] + t_r. \tag{41}$$

The system phase trajectory is shown in Fig. 5. It can be inferred from the trajectory that for any arbitrarily initial point, the tracking error converges to zero within a finite time.

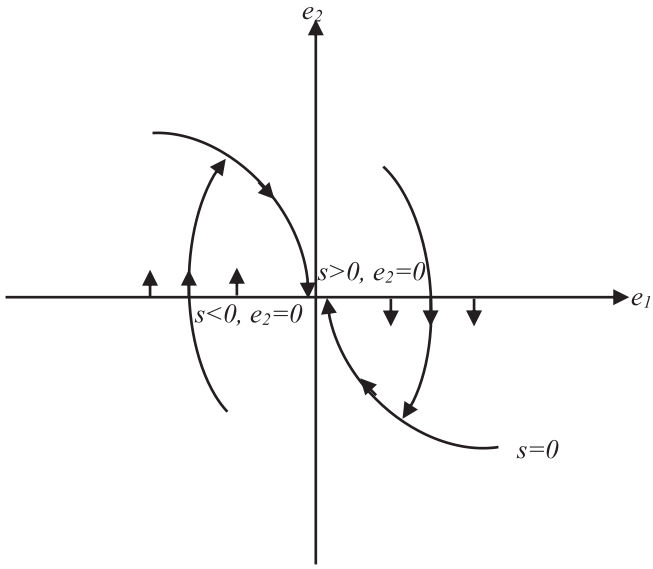

Fig. 5. Phase trajectory of the system.

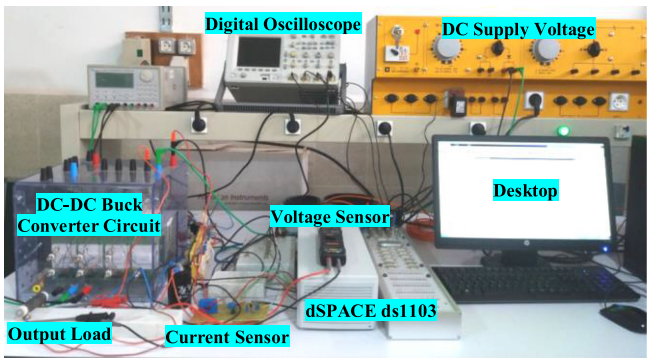

Fig. 6. Experimental setup of the dc–dc buck converter.

V. Experimental Study

The laboratory experimental platform, shown in Fig. 6, includes a dc–dc buck converter designed to work in CCM at a switching frequency of 10 kHz. A pair of sensors was devised for measuring the output capacitor voltage and the current that passes through the inductor. An additional circuit allowed enable/disable a disturbance resistive load triggered by a manual switch. The control algorithm, the PWM generation and the desired reference trajectory were implemented using a TMS320F28335 microprocessor (Texas Instruments Inc., USA), a DSP board DS1103 (dSPACE, Inc., Germany) and the MATLAB/Simulink program. The complete scheme operates at a fixed sampling rate of 25 kHz.

Some experimental tests are established to show and compare the benefits of all designed controllers: 1) NTSMC control scheme with saturation function; 2) FO-NTSMC control scheme with continuous function, and 3) proposed AFFO-NTSMC control scheme, particularly in presence of various sources of disturbances rejection and parametric uncertainties. The following tests are performed in the dc–dc buck converter: Test 1: Start-up response (0—30 V), Test 2: Step-load waveforms, Test 3: Reference trajectory tracking, Test 4: Sinusoidal-wave tracking, Test 5: Triangular-wave tracking. The nominal parameters of the dc–dc buck converter are selected as follows: $L = 5$ mH, $C = 1100$ μF, $R = 82$-36 Ω, and $v_{in} = 75$ V. The important control parameters are chosen as: $\frac{1}{\rho} = 0.02$, $\lambda = 1.66$, $K_1 = 0.058$, $K_2 = 0.8$; $H^* = 100$; $\alpha = 0.5$.

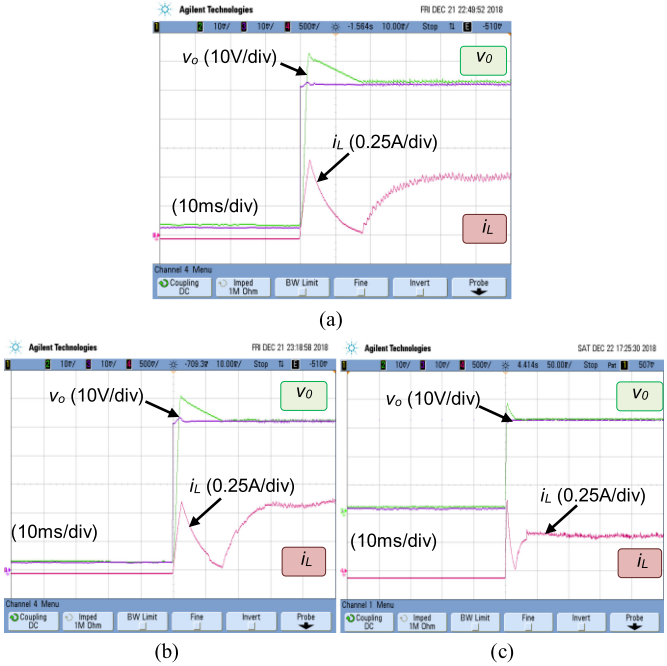

Fig. 7. Experimental results of output voltage v_0 and inductor current i_L for a nominal start-up response in the output voltage reference using (a) NTSMC algorithm, (b) FO-NTSMC algorithm, and (c) proposed AFFO-NTSMC algorithm.

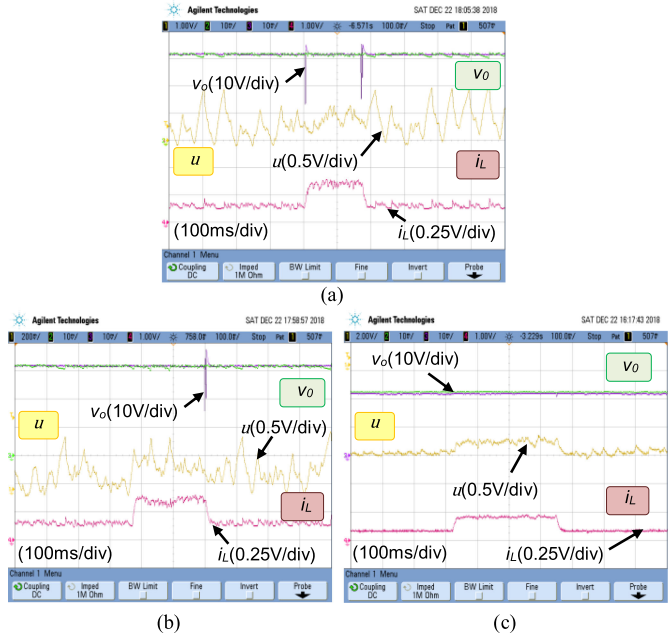

Fig. 8. Experimental results of output voltage v_0 inductor current i_L and duty ratio u for a step-load responses using (a) NTSMC algorithm, (b) FO-NTSMC algorithm, and (c) proposed AFFO-NTSMC algorithm.

A. Test 1: Start-Up Response (0—50 V)

The performance of the aforementioned control strategies in regulating the output voltage v_o, at a start-up response (0—50 V), is tested under the normal conditions. The resulting variations in output voltage v_o and inductive current i_L, exhibited by each of the three controllers are shown in Fig. 7(a)–(c), respectively. It is clear that the overshoot under the proposed AFFO-NTSMC controller is lower than that under the other two control strategies (NTSMC and FO-NTSMC), since the proposed AFFO-NTSMC control law uses the fractional-order and the adaptive control techniques. The rise-time of the start-up response under the proposed FO-NTSMC controller is approximately 7 ms, which is shorter than that under the other two control strategies, with the corresponding times of 17 ms and 15 ms when comparing with the NTSMC and FO-NTSMC control strategies, respectively. In addition, the settling-time under the proposed AFFO-NTSMC controller is less than 5 ms, whereas it is greater than 15 ms in NTSMC and close to 12 ms in the FO-NTSMC controller, respectively. So, the proposed AFFO-NTSMC strategy can slightly improve the reaching and settling-time of the start-up response in terms of the voltage adjustment.

B. Test 2: Step-Load Waveforms

Experimental step-load waveforms of the output voltage v_o, duty ratio u, and inductive current i_L between these three control lows, when the load resistance steps from nominal value of 82 to 36 Ω and vice-versa are shown in Fig. 8(a)–(c), respectively. Note from Fig. 8(c) that during the strong load resistance variations, the proposed AFFO-NTSMC algorithm ensures zero steady-state error in the output voltage, with only a slight decrease in voltage ripples around the output voltage reference value. Also, it is observed that the voltage fluctuations under the proposed AFFO-NTSMC algorithm are not presented in the recorded output voltage response. Compared with two other control algorithms, the voltage fluctuations are clearly visible when the NTSMC and FO-NTSMC algorithms are implemented to deal with the presence of perturbations from components uncertainties. The output voltage recovery-time under the proposed AFFO-NTSMC algorithm is approximately 5 ms, which is fast than that under the other two control algorithms, with the corresponding times of 20 and 10 ms when comparing with the NTSMC and FO-NTSMC control algorithms, respectively. The different voltage fluctuation and recovery-time are caused by the different sliding surface design of the three aforementioned control algorithms.

C. Test 3: Reference Trajectory Tracking Performance

Here, each controller is applied to the dc–dc buck converter to study the performance of reference tracking during a step change in the output voltage reference from $v_{ref} = 30$ to 50 V and then to 30 V. The tracking performance of the output voltage v_o and inductive current i_L under three control algorithms are depicted in Fig. 9(a)–(c), respectively. As shown in these figures, the tracking response of the proposed AFFO-NTSMC algorithm is acceptable in both the transient and the steady-state responses. Moreover, the tracking is offset-free. For comparison with NTSMC and FO-NTSMC algorithms, it is obvious that the tracking responses of both controllers have offsets, but the NTSMC algorithm shows slightly better performance, since

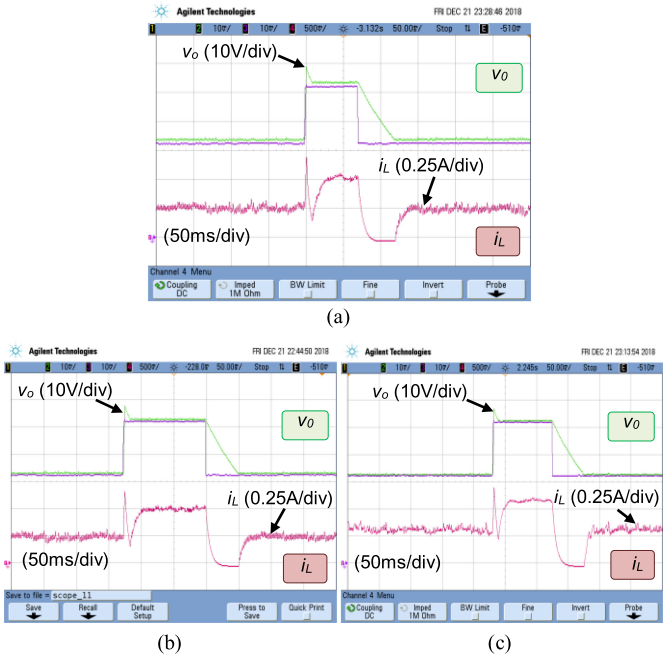

Fig. 9. Experimental results of output voltage v_0 and inductor current i_L for a step-up change in the output voltage reference using (a) NTSMC algorithm, (b) FO-NTSMC algorithm, and (c) proposed AFFO-NTSMC algorithm.

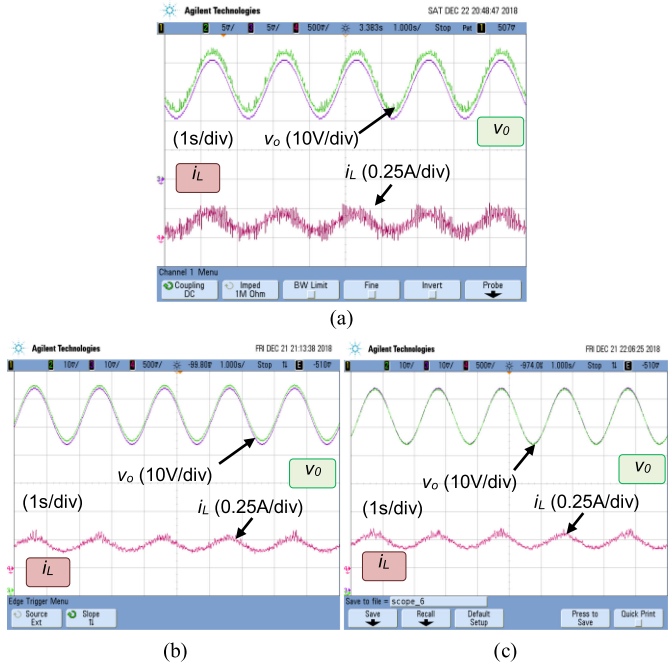

Fig. 10. Experimental results of output voltage v_0 and inductor current i_L for a sinusoidal-wave tracking in the output voltage reference using (a) NTSMC algorithm, (b) FO-NTSMC algorithm, and (c) proposed AFFO-NTSMC algorithm.

it has slightly better accuracy and speed in response to the reference trajectory tracking.

D. Test 4: Sinusoidal-Wave Tracking Performance

The trajectory tracking performance of each control algorithm is tested by applying a sinusoidal-wave reference output voltage. The corresponding response of v_o and i_L under the influence of each control algorithm is illustrated in Fig. 10(a), (b), and (c), respectively. As can be seen from these figures, the proposed AFFO-NTSMC algorithm not only provides more accurate results but also increases the convergence speed of the buck converter and reduces the chattering phenomena. Specifically, the AFFO-NTSMC algorithm delivers the smallest tracking errors among the three controllers. Comparing Fig. 10(c) with (a) and (b), we can observe that the NTSMC algorithm produces significant chattering phenomena due to the control input action around the sliding surfaces. The FO-NTSMC can considerably reduce the chattering. However, there is a tradeoff between chattering reduction and tracking performance. At the same time, the AFFO-NTSMC algorithm attenuated chattering, while achieving small tracking errors with a significantly improved transient and steady-state response.

E. Test 5: Triangular-Wave Tracking Performance

The trajectory tracking performance of each control algorithm is tested by applying a triangular-wave reference output voltage. The reference voltage oscillates between $+15.0$ and $+55.0$ V as a ramp. The oscillation frequency of the reference voltage is set to 0.1 Hz. The corresponding disturbances occurring in the response of v_o and i_L under the influence of each of the three controllers are illustrated in Fig. 11(a)–(c), respectively. The graphical responses confirm the superiority of the trajectory tracking performance exhibited by the AFFO-NTSMC algorithm over the NTSMC and FO-NTSMC algorithms.

The NTSMC algorithm's response exhibits a significant tracking error. The response of FO-NTSMC algorithm consistently lags behind the reference trajectory by 0.1 s while tracking it. The proposed AFFO-NTSMC algorithm's response accurately tracks the trajectory with negligible lag and minimal tracking error.

F. Comparison Analysis and Summary

To officially compare the controllers in a useful manner, qualitative performance criteria are very useful. They are extensively used in the literature for comparison purpose.

In this article, three criteria have been favored namely: rise-time t_r, settling-time t_s, and percentage of over-shoot or under-shoot M_p %. Table I summarized the comparison between the qualitative performances of the three synthesized controllers.

The aforementioned qualitative comparison has confirmed that the proposed AFFO-NTSMC control law owns the optimum performance on the dc–dc buck platform. To make the conclusion more realistic, we perform the quantitative analysis and comparison using the statistics of the steady experimental data. The average precision of the tracking performance can be found from the definition of root-mean-square error $e_{\rm rms}$ as

$$e_{\rm rms} = \sqrt{\sum_{i=1}^{N} \frac{(x(i) - x_d(i))^2}{N}} \tag{42}$$

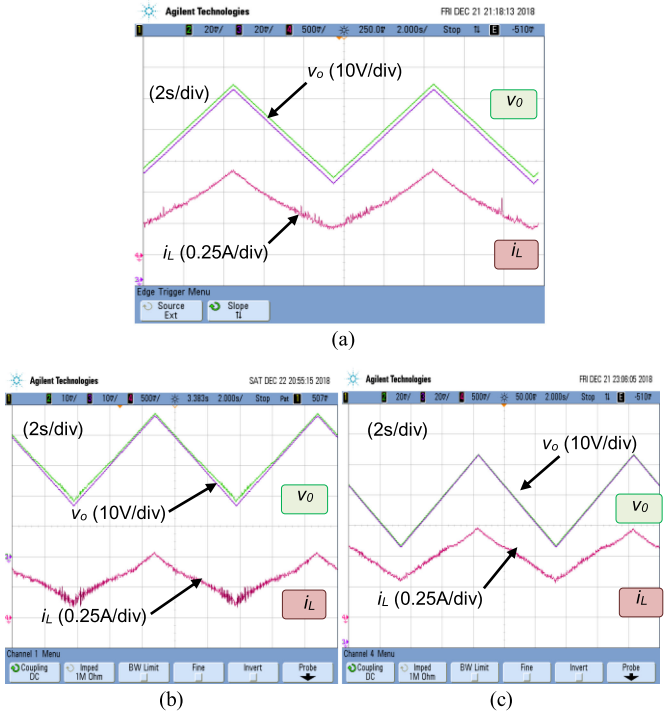

Fig. 11. Experimental results of output voltage v_0 and inductor current i_L for a triangular-wave tracking in the output voltage reference using (a) NTSMC algorithm, (b) FO-NTSMC algorithm, and (c) proposed AFFO-NTSMC algorithm.

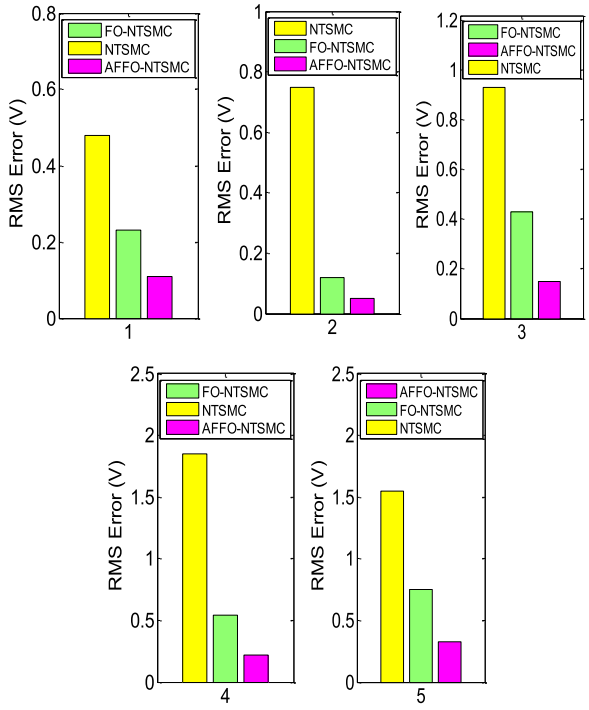

Fig. 12. RMS profile of the tracking error under all experimental tests.

TABLE I
COMPARISON BETWEEN THE NTSMC, FO-NTSMC, AND AFFO-NTSMC

Test	Controllers	t_r[ms]	t_s[ms]	M_p[%]
1	NTSMC[53]	15.72	17	25
	FO-NTSMC	11.25	15	20
	AFFO-NTSMC	4.54	6.88	5
2	NTSMC[53]	18.20	20	56
	FO-NTSMC	8.33	10	45
	AFFO-NTSMC	3.15	4.75	0.33
3	NTSMC[53]	0.54	1.15	18
	FO-NTSMC	0.41	0.97	15
	AFFO-NTSMC	0.21	0.10	10
4	NTSMC[53]	-	-	9
	FO-NTSMC	-	-	4
	AFFO-NTSMC	-	-	0.10
5	NTSMC[53]	-	-	6
	FO-NTSMC	-	-	2
	AFFO-NTSMC	-	-	0.10

where N is the sample number at which the rms value is calculated. A ten samples are used to evaluate the rms value. The results of rms profile of the tracking error in all the experimental tests are displayed as bar charts in Fig. 12. From this figure, we can say that the proposed AFFO-NTSMC control law is the best performing one among the other two algorithms. The FO-NTSMC control algorithm takes the second position, which implies that the tracking accuracy benefits from the introduction of fractional integration into the controller design. Thus, the results indicate that the proposed AFFO-NTSMC control algorithm can be applied to the dc–dc buck converter control, and guarantees a good response and high accuracy tracking performance with noticeable robustness against disturbances and parameters variations.

VI. CONCLUSION

This article has presented the design of a robust AFFO-NTSMC algorithm for an uncertain dc–dc buck converter, in which the output voltage is required to track a desired rest-to-rest voltage profile. The dc–dc buck converter model includes time-varying parameters, represented by the output load resistance. In order to establish the AFFO-NTSMC algorithm, a new fractional-order nonsingular terminal sliding mode surfaces were proposed. Also, based on the adaptive interval type-1 fuzzy system, Lyapunov stability criteria, and finite-time control method, the proposed AFFO-NTSMC algorithm has been designed. The chattering-free is ensured even though the proposed AFFO-NTSMC algorithm operates under the presence of external disturbances and uncertainties, as well as the finite-time stability of the closed-loop system is rigorously guaranteed by the proposed controller. The effectiveness of the AFFO-NTSMC algorithm was successfully tested on a laboratory dc–dc buck converter prototype subject to resistive load variations. The performed tests for offset-free reference tracking as well as disturbance rejection on the output voltage regulating have transparently demonstrated the robustness and the high dynamic capability of the AFFO-NTSMC algorithm over the NTSMC and FO-NTSMC algorithms. In summary, the proposed AFFO-NTSMC algorithm promises to be perfectly suitable for practical applications of dc–dc buck converters.

REFERENCES

[1] C. M. Lai, Y. H. Cheng, M. H. Hsieh, and Y. Lin, "Development of a bidirectional DC/DC converter with dual-battery energy storage for hybrid electric vehicle system," *IEEE Trans. Veh. Technol.*, vol. 67, no. 2, pp. 1036–1052, Feb. 2018.

[2] J. Wang, S. Li, J. Yang, B. Wu, and Q. Li, "Extended state observer-based sliding mode control for PWM-based DC–DC buck power converter systems with mismatched disturbances," *IET Control Theory Appl.*, vol. 9, no. 4, pp. 579–586, 2015.

[3] A. S. Oshaba, E. S. Ali, and S. M. Abd-Elazim, "ACO based speed control of SRM fed by photovoltaic system," *Int. J. Electr. Power Energy*, vol. 67, pp. 529–536, 2015.

[4] A. S. Oshaba, E. S. Ali, and S. M. Abd-Elazim, "MPPT control design of PV system supplied SRM using BAT search algorithm," *Sustain. Energy Grids Netw.*, vol. 2, pp. 51–60, 2015.

[5] V. S. C. Racirah and P. C. Sen, "Comparative study of proportional-integral, sliding mode, and fuzzy logic controllers for power converters," *IEEE Trans. Ind. Appl.*, vol. 33, no. 1, pp. 518–524, Mar./Apr. 1997.

[6] C. L. Zhang, J. X. Wang, S. H. Li, B. Wu, and C. Qian, "Robust control for PWM-based DC-DC buck power converters with uncertainty via sampled-data output feedback," *IEEE Trans. Power Electron.*, vol. 30, no. 1, pp. 504–515, Jan. 2015.

[7] B. Amir and M. Dragan, "Hybrid digital adaptive control for fast transient response in synchronous buck DC-DC converters," *IEEE Trans. Power Electron.*, vol. 24, no. 11, pp. 2625–2638, Nov. 2009.

[8] V. Yousefzadeh, A. Babazadeh, B. Ramachandran, E. Alarcon, L. Pao, and D. Maksimovic, "Proximate time-optimal digital control for synchronous buck DC-DC converters," *IEEE Trans. Power Electron.*, vol. 23, no. 4, pp. 2018–2026, Jul. 2008.

[9] B. Babes, A. Boutaghane, N. Hamouda, and M. Mezaache, "Design of a robust voltage controller for a DC–DC buck converter using fractional-order terminal sliding mode control strategy," in *Proc. Int. Conf. Adv. Elect. Eng.*, Algiers, Algeria, Nov. 2019, pp. 1–6. [Online]. Available: https://doi.org/10.1109/ICAEE47123.2019.90147 88

[10] R. Silva-Ortigoza, V. Hernndez-Guzmn, M. Antonio-Cruz, and D. Muoz-Carrillo, "DC/DC buck power converter as a smooth starter for a DC motor based on a hierarchical control," *IEEE Trans. Power Electron.*, vol. 30, no. 2, pp. 1076–1084, Feb. 2015.

[11] B. Babes, A. Boutaghane, and N. Hamouda, "Design and real-time implementation of an adaptive fast terminal synergetic controller based on dual RBF neural networks for voltage control of DC–DC step-down converter," *Elect. Eng.*, Jul. 2021. [Online]. Available: https://doi.org/10.1007/s00202-021-01353-y

[12] D. Maria, P. Marcello, and R. Antoella, "Analytical versus neural real-time simulation of a photovoltaic generator based on a DC-DC converter," *IEEE Trans. Ind. Appl.*, vol. 46, no. 6, pp. 2501–2510, Nov./Dec. 2010.

[13] D. B. W. Abeywardana, B. Hredzak, and V. G. Agelidis, "A fixed-frequency sliding mode controller for a boost-inverter-based battery-supercapacitor hybrid energy storage system," *IEEE Trans. Power Electron.*, vol. 32, no. 1, pp. 668–680, Jan. 2016.

[14] C. Mu and H. He, "Dynamic behavior of terminal sliding mode control," *IEEE Trans. Ind. Electron.*, vol. 65, no. 4, pp. 3480–3490, Apr. 2018, doi: 10.1109/TIE.2017.2764842.

[15] A. T. Vo and H. J. Kang, "A chattering-free, adaptive, robust tracking control scheme for nonlinear systems with uncertain dynamics," *IEEE Access*, vol. 7, pp. 10457–10466, Jan. 2019.

[16] S.-C. Tan, Y. M. Lai, M. K. H. Cheung, and C. K. Tse, "On the practical design of a sliding mode voltage controlled buck converter," *IEEE Trans. Power Electron.*, vol. 20, no. 2, pp. 425–437, Mar. 2005, doi: 10.1109/TPEL.2004.842977.

[17] Y. Yang, K. Mok, S. Tan, and S. Y. Hui, "Nonlinear dynamic power tracking of low-power wind energy conversion system," *IEEE Trans. Power Electron.*, vol. 30, no. 9, pp. 5223–5236, Sep. 2015, doi: 10.1109/TPEL.2014.2363561.

[18] Y. Mao and Y. Yang, "A double-integral sliding mode-based hybrid control for a single-input-multiple-output buck converter," *IEEE J. Emerg. Sel. Topics Ind. Electron.*, vol. 2, no. 3, pp. 247–256, Jul. 2021, doi: 10.1109/JESTIE.2021.3051588.

[19] R. Ling, D. Maksimovic, and R. Leyva, "Second-order sliding-mode controlled synchronous buck DC–DC converter," *IEEE Trans. Power Electron.*, vol. 31, no. 3, pp. 2539–2549, Mar. 2016, doi: 10.1109/TPEL.2015.2431193.

[20] S. Ding, W. X. Zheng, J. Sun, and J. Wang, "Second-order sliding-mode controller design and its implementation for buck converters," *IEEE Trans. Ind. Informat.*, vol. 14, no. 5, pp. 1990–2000, May 2018, doi: 10.1109/TII.2017.2758263.

[21] Z. Wang, S. Li, and Q. Li, "Discrete-time fast terminal sliding mode control design for DC–DC buck converters with mismatched disturbances," *IEEE Trans. Ind. Informat.*, vol. 16, no. 2, pp. 1204–1213, Feb. 2020, doi: 10.1109/TII.2019.2937878.

[22] H. Komurcugil, "Adaptive terminal sliding-mode control strategy for DC-DC buck converters," *ISA Trans.*, vol. 51, no. 6, pp. 673–681, 2012.

[23] D. Zhao, S. Li, and F. Gao, "A new terminal sliding mode control for robotic manipulators," *Int. J. Control*, vol. 82, pp. 1804–1813, 2009.

[24] H. Komurcugil, "Non-singular terminal sliding-mode control of DC–DC buck converters," *Control Eng. Pract.*, vol. 21, no. 3, pp. 321–332, 2013.

[25] M. Jin, J. Lee, P. H. Chang, and C. Choi, "Practical nonsingular terminal sliding-mode control of robot manipulators for high-accuracy tracking control," *IEEE Trans. Ind. Electron.*, vol. 56, no. 9, pp. 3593–3601, Sep. 2009.

[26] L. Qiao and W. Zhang, "Adaptive non-singular integral terminal sliding mode tracking control for autonomous underwater vehicles," *IET Control Theory Appl.*, vol. 11, no. 8, pp. 1293–1306, 2017.

[27] J. Tsai and Y. Chen, "Sliding mode control and stability analysis of buck DC-DC converter," *Int. J. Electron.*, vol. 94, pp. 209–222, 2007.

[28] R. D. Al-Dabbagh, A. Kinsheel, S. Mekhilef, M. S. Baba, and S. Shamshirband, "System identification and control of robot manipulator based on fuzzy adaptive differential evolution algorithm," *Adv. Eng. Softw.*, vol. 78, pp. 60–66, 2014.

[29] O. Barambones, P. Alkorta, A. J. Garrido, I. Garrido, and F. J. Maseda, "An adaptive sliding mode control scheme for induction motor drives," *Int. J. Circuits, Syst. Signal Process.*, vol. 1, pp. 73–79, 2007.

[30] F. Qiao, Q. Zhu, A. Winfield, and C. Melhuish, "Adaptive sliding mode control for MIMI nonlinear systems based on a fuzzy logic scheme," *Int. J. Automat. Comput.*, vol. 1, pp. 51–62, 2004.

[31] C. C. Yang, "Robust adaptive terminal sliding mode synchronized control for a class of non-autonomous chaotic systems," *Asian J. Control*, vol. 15, no. 6, pp. 1677–1685, 2013.

[32] C. K. Lin, "Nonsingular terminal sliding mode control of robot manipulators using fuzzy wavelet networks," *IEEE Trans. Fuzzy Syst.*, vol. 14, no. 6, pp. 849–859, Dec. 2006.

[33] J. Fei, W. Yan, and Y. Yang, "Adaptive nonsingular terminal sliding mode control of MEMS gyroscope based on backstepping design," *Int. J. Adaptive Control Signal Process.*, vol. 29, no. 9, pp. 1099–1115, 2015.

[34] D. Lei and J. Fei, "Adaptive neural nonsingular terminal sliding mode control for MEMS gyroscope based on dynamic surface controller," *Int. J. Mach. Learn. Cybern.*, vol. 9, pp. 1285–1295, 2017.

[35] T. Aounallah, N. Essounbouli, A. Hamzaoui, and F. Bouchafaa, "Algorithm on fuzzy adaptive backstepping control of fractional order for doubly-fed induction generators," *IET Renewable Power Gener.,* vol. 12, no. 8, pp. 962–967, 2018.

[36] Y. Li, Y. Q. Chen, and H. S. Ahn, "Fractional-order iterative learning control for fractional-order linear systems," *Asian J. Control*, vol. 13, pp. 54–63, 2011.

[37] X. Dingyu, Z. Chunna, and C. Yang Quan, "Fractional order PID control of a DC-motor with elastic shaft: A case study," in *Proc. IEEE Amer. Control Conf. Hilton Minneapolis Hotel*, Minneapolis, MN, USA, Jun. 2006, pp. 3182–3187.

[38] S. Karad, S. Chatterji, and P. Suryawanshi, "Performance analysis of fractional order PID controller with the conventional PID controller for bioreactor control," *Int. J. Sci. Eng. Res.*, vol. 3, no. 6, pp. 1–6, 2012.

[39] H. Malek, S. Dadras, and Y. Q. Chen, "An improved maximum power point tracking based on fractional order extremum seeking control in grid-connected photovoltaic (PV) systems," in *Proc. ASME Int. Des. Eng. Tech. Conf. Comput. Inf. Eng. Conf.,* Amer. Soc. Mech. Eng., Portland, OR, USA, 2013, vol. 4–7, Art. no. V004T08A024.

[40] I. N'Doye *et al.*, "Static output feed-back HN control for a fractional-order glucose-insulin system," *Int. J. Control, Automat. Syst.*, vol. 13, pp. 798–807, 2015.

[41] Z. Bingul and O. Karahan, "Tuning of fractional PID controllers using PSO algorithm for robot trajectory control," in *Proc. IEEE Int. Conf. Mechatronics*, Istanbul Technical University, Istanbul, Turkey, Aug. 2011, pp. 955–960.

[42] L. Chen, R. Wu, Y. He, and Y. Chai, "Adaptive sliding-mode control for fractional-order uncertain linear systems with non-linear disturbances," *Nonlinear Dyn.*, vol. 80, no. 1/2, pp. 51–58, 2015.

[43] C. Yin and S. Dadras, "Control of a novel class of fractional-order chaotic systems via adaptive sliding mode control approach," *Appl. Math. Model.*, vol. 37, no. 4, pp. 2469–2483, 2013.

[44] T. Lin and T. Lee, "Adaptive fuzzy sliding mode control for synchronization of uncertain fractional order chaotic systems," *Chaos Solitons Fractals*, vol. 44, no. 10, pp. 791–801, 2011.
[45] D. Nojavanzadeh and M. Badamchizadeh, "Adaptive fractional-order nonsingular fast terminal sliding mode control for robot manipulators," *IET Control Theory Appl.*, vol. 10, no. 13, pp. 1565–1572, 2016.
[46] M. Ö. Efe, "Fractional fuzzy adaptive sliding-mode control of a 2-DOF direct-drive robot arm," *IEEE Trans. Syst., Man, Cybern. , B (Cybern.)*, vol. 38, no. 6, pp. 1561–1570, Dec. 2008.
[47] J. Fei and C. Lu, "Adaptive fractional order sliding mode controller with neural estimator," *J. Franklin Inst.*, vol. 355, no. 5, pp. 2369–2391, 2018.
[48] B. Babes *et al.*, "New optimal control of permanent magnet dc motor for photovoltaic wire feeder systems," *J. Européen des Systèmes Automatisés*, vol. 53, no. 6, pp. 811–823, Dec. 2020. [Online]. Available: https://doi.org/10.18280/jesa.530607
[49] N. Hamouda, B. Babes, C. Hamouda, S. Kahla, T. Ellinger, and J. Petzoldt, "Optimal tuning of fractional order proportional-integral-derivative controller for wire feeder system using ant colony optimization," *J. Européen des Systèmes Automatisés*, vol. 53, no. 2, pp. 157–166, Apr. 2020. [Online]. Available: https://doi.org/10.18280/jesa.530201
[50] S. Kahla, M. Bechouat, T. Amieur, M. Sedraoui, B. Babes, and N. Hamouda, "Maximum power extraction framework using robust fractional-order feedback linearization control and GM-CPSO for PMSG-basedWECS," *Wind Eng.*, vol. 45, no. 4, pp. 1040–1054, 2020, doi: 10.1177/0309524X20948263.
[51] B. Babes, A. Boutaghane, H. Hamouda, M. Mezaache, and S. Kahla, "A robust adaptive fuzzy fast terminal synergetic voltage control scheme for DC/DC buck converter," in *Proc. Int. Conf. Adv. Elect. Eng.*, Algiers, Algeria, Nov. 2019, pp. 1–5. [Online]. Available: https://doi. org/10.1109/ICAEE47123.2019.9014717
[52] N. Hamouda and B. Babes, "A DC/DC buck converter voltage regulation using an adaptive fuzzy fast terminal synergetic control," in *Proc. 4th Int. Conf. Elect. Eng. Control Appl.*, Singapore, vol. 682, pp. 711–721, Sep. 2020. [Online]. Available: https://doi.org/10.1007/978-981-15-6403-1_48
[53] B. Wang, G. Ma, D. Xu, L. Zhang, and J. Zhou, " Switching sliding-mode control strategy based on multi-type restrictive condition for voltage control of buck converter in auxiliary energy source," *Appl. Energy*, vol. 228, pp. 1373–1384, 2018.

Badreddine Babes received the B.Eng. and M.Sc. degrees in electrical engineering and the Doctorate degree in electrical engineering (*with specialization in electric drive applications and controls*) from the University of Setif-1, Setif, Algeria, in 2004, 2010, and 2018, respectively.

He was with Research Center in Industrial Technologies (CRTI), Algiers, Algeria, in 2017 as Assistant Researcher and he is currently with the CRTI as Senior Researcher "A". His research interests include power electronic converters, active power filters, and renewable energy.

Saad Mekhilef (Senior Member, IEEE) received the B.Eng. degree in electrical engineering from the the University of Setif, Setif, Algeria, in 1995, and the Master of Engineering Science and Ph.D. degrees from University of Malaya, Kuala Lumpur, Malaysia, in 1998 and 2003, respectively.

He is currently a Distinguished Professor with the School of Science, Computing and Engineering Technologies, Swinburne University of Technology, Australia and Honorary Professor with the Department of Electrical Engineering, University of Malaya. He has authored and coauthored more than 400 publications in academic journals and proceedings and five books with more than 30 000 citations. He is actively involved in industrial consultancy, for major corporations in the power electronics projects. His research interests include power conversion techniques, control of power converters, renewable energy, and energy efficiency.

Amar Boutaghane received the B.Eng. and M.Sc. degrees in optics and mechanics of precision from the University of Setif, Setif, Algeria, in 1996 and 2000, respectively, and the Ph.D. degree in mechanical engineering from the University of Algiers, Algiers. Algeria, in 2012.

He was with Research Center in Industrial Technologies (CRTI), Algiers, Algeria in 2002, as an Assistant Researcher, and he is currently with the CRTI as the Head of Research Division of Welding and Allied Process. His research interests include plasma modeling, plasma arc, and welding.

Lazhar Rahmani received the Engineering degree in electrical engineering from the University of Annaba, Annaba, Algeria, in 1991, and the D.E.A. and Ph.D. degrees from the University of Setif-1, Setif, Algeria, in 1994 and 2005, respectively, all in electrical engineering.

He is currently an Assistant Professor with the Department of Electrical Engineering, University of Setif-1, Algeria. His current research interests include modeling and advanced control of power converters and power electronic systems and their digital control techniques.